On-Chip Optical Vector Quadrature De-Multiplexer Proposal for QAM De-Aggregation by Single Bi-Directional SOA-Based Phase-Sensitive Amplifier

JIABIN CUI[1], **(Student Member, IEEE), GUO-WEI LU**[2,3], **(Member, IEEE),**
HONGXIANG WANG[1], **(Member, IEEE), AND YUEFENG JI**[1], **(Senior Member, IEEE)**

[1]State Key Laboratory of Information Photonics and Optical Communications, School of Information and Communication Engineering, Beijing University of Posts and Telecommunications, Beijing 100876, China
[2]Institute of Innovative Science and Technology, Tokai University, Kanagawa 259-1292, Japan
[3]National Institute of Information and Communications Technology, Tokyo 184-8795, Japan

Corresponding author: Yuefeng Ji (jyf@bupt.edu.cn)

ABSTRACT In this paper, a simple optical vector quadrature de-multiplexer (QD) scheme is proposed for de-aggregating input 10 Gbaud 16/32/64 quadrature amplitude modulation (QAM) signals into two pulse amplitude modulation (PAM) streams. The proposed QD is based on a single bi-directional degenerate phase-sensitive amplifier (PSA), where the wavelength and the polarization status of the extracted in-phase and quadrature components stay the same as the input signal. Since the proposed QD is realized using PSA based on semiconductor optical amplifier (SOA), it is also possible to realize an on-chip QD system, providing an integrated platform for optical signal processing. Through numerical simulation, the transfer characteristics of the proposed QD system show that the SOA-based PSA has a high phase-sensitive gain extinction ratio of 44.1 dB. The constellations, error vector magnitudes (EVMs), and bit-error rates (BERs) of the data streams after the de-aggregation are numerically investigated to verify the proposed QD scheme. For the 10 Gbaud 16/32/64 QAM signals with an input optical signal-to-noise ratio (OSNR) of 25 dB, the de-aggregated PAM4/PAM6/PAM8 signals show 6.1, 5.6, and 8.2 dB receiver OSNR improvements at the BER of 10^{-3}, respectively. Also, to optimize the performance of the subsystem, the BER performance dependence on the phase difference between two arms in the subsystem is also examined. The simulation results reveal that the proposed QD can accomplish the function of optical vector de-aggregation well for the high-level QAM signals. The proposed QD can be applied to information de-aggregation, format conversion, and direct detection for optical vector signals, which may have great potential values for the flexible optical networks.

INDEX TERMS Optical fiber communication, nonlinear optical devices, optical signal processing, semiconductor optical amplifiers.

I. INTRODUCTION

The approaching of the 5th generation (5G) mobile network forcefully propels the optical network to optimize its network architecture and critical performances such as the network capacity, efficiency, time-delay and flexibility [1]. Among these demands, extending the capacity is a particularly urgent and persistent issue. Multi-dimensional all-optical network (AON) is proposed to relieve the capacity pressure by employing multiple multiplexing technologies and high-order modulation formats [2]. In long-haul networks, the optical vector signals are employed and manipulated in domains of amplitude, phase, wavelength and polarization to improve the transmission capacity and spectral efficiency (SE) [3] like the wavelength division multiplexing dual-polarization quadrature amplitude modulation (WDM DP-QAM) signals. The QAM signals can effectively promote the transmission SE and are extensively researched in over 400G transmission [4]–[6]. Apart from the ultra-large capacity transmission schemes, all-optical signal processing for QAMs is also important to support the QAM-based

AON and various processing applications for QAM have been proposed such as wavelength converting [7], add/drop multiplexing [8], lossless optical switches [9] and low-noise amplification [10], [11].

The QAM signals are usually generated by in-phase and quadrature (IQ) modulation which means the optical vector is two-dimensional and the data information is carried by its I and Q components. All-optical quadrature de-multiplexing is a crucial signal processing function which can extract I and Q components of input optical vector and has vast potential applications like format conversion, information de-aggregation and signal detection. Phase-sensitive amplifier (PSA) has great advantage in processing the optical vector signals for its unique phase-sensitive characteristic and various PSA based optical quadrature de-multiplexer (QD) schemes have been proposed. The idea of PSA based QD is proposed by [12] while it can extract only one quadrature of input optical vector at a time. The schemes proposed in [13] and [14] extract the two quadratures of input QPSK vector simultaneously at different wavelengths and polarizations, respectively. With the higher-level modulation formats being commercial progressively, the researches about PSA based QD also aim at higher-level QAM signals. The QDs in [15] and [16] de-aggregate 16QAM signals and the extracted I and Q components are also assigned to different wavelengths and polarizations, respectively. Moreover, the quadrature de-multiplexing for two wavelength channels 16QAM signals is accomplished by [17] and the output components are distinguished by wavelength. Though these schemes realize the de-aggregation for QAM vectors, the different wavelengths or polarizations for the extracted components will bring inconvenience to the following signal transmission or processing. It is a key issue for the optical quadrature de-multiplexing to make the extracted I and Q components keep the same wavelength and polarization status with the input signal. The QD proposed in [18] de-aggregates one DP-QPSK into two DP-BPSKs and avoids this problem while it has a complicated QD structure and requires a strict polarization relation among the input QPSK and pump waves.

Another critical issue for the current QD schemes is the system integration. We can see that the nonlinear optical medium employed by the current QD are usual high nonlinear fiber (HNLF) which is difficult to be integrated. While most of the signal processors have strict requirements for the inner link coherence which means the environment issues like acoustic and thermal effects [19] have serious influences on the processing effect. The optical devices integration is a very effective approach to solve this problem and various basic optical devices are realized on a chip like optical coupler [20], optical filter [21], optical circulator [22] and wavelength multiplexer [24] which can be basic modules to accomplish some more complicated on-chip optical signal processors and functions like optical digital operations [25], optoelectronic oscillator [26], optical frequency combs [27] and logic gates [28]. For the ultra-small footprint, high reliability and

high power efficiency, the integrated optical devices draw research attentions and are regarded as the future trend for the all-optical signal processors.

We have proposed a bi-directional PSA based QD scheme in [29] and apply it into the de-aggregation for 16 and 64QAM signals. The bi-directional PSA-based QD has a simple system setup and ensures the output I and Q components have the same wavelength and polarization with the input QAM signals while it also employs one HNLF to be the nonlinear medium. To investigate the possibility for on-chip solution of QD system, we replace the HNLF in [29] by a semiconductor optical amplifier (SOA), a universal and mature on-chip nonlinear optical device in practical. There have been proposed SOA-based PSA systems which are demonstrated to be with phase-sensitive characteristics [30], [31] or as regenerators [32], [33]. These proposals indicate the integration possibility for PSA while the SOA-based QD system has not been put forward. The constructing devices of our proposed QD system like SOA, coupler, optical filter and wavelength multiplexer are all ready for on-chip integration, the integrated circulator has also been demonstrated based on silica micro-resonator [22], so the study in this paper provides a possible on-chip solution for the optical vector QD.

In this paper, a single bi-directional PSA based optical vector QD is proposed and the de-aggregations for 10 Gbaud 16/32/64 QAM signals are performed. The wavelength and polarization status of the extracted I and Q components are maintained to be the same with the input QAM signal. Moreover, we choose a SOA to be the nonlinear optical medium of PSA to verify the on-chip QD solution. The QD system transfer characteristics are investigated, and the results show that the QD has a high phase-sensitive gain extinction ratio of 44.1 dB in both I and Q branches. For the de-aggregation of input 10 Gbaud 16/32/64 QAM signals, the constellations, error vector magnitude (EVM) and bit-error rate (BER) of the signals before and after the QD are investigated to evaluate the system performance. Comparing with the input 16/32/64 QAM signals, 6.1 dB, 5.6 dB and 8.2 dB receiver optical signal-to-noise ratio (OSNR) improvement are gained by the extracted four-level pulse amplitude modulation (PAM4)/PAM6/PAM8 at the BER of 10^{-3}, respectively. The effect of path phase difference on the system BER and the performance difference between I and Q components are also analyzed by the BER performance factor (BPF) which is used to evaluate the BER performance for the signal with different path phase differences. In the following sections, the detailed theoretical derivations, system simulations and performances discussion are presented.

II. OPERATION PRINCIPLE

The optical vector signals like QAM signals are generated by two-dimensional modulation in order to carry the data information on the I and Q parts of the signal. The optical QD is to de-aggregate the optical vector into I and Q parts separately. In this section, we will introduce the concept of

quadrature de-multiplexing for optical vector and the operation principle of our proposed on-chip QD.

An optical vector in transmission systems can be mathematically viewed as the multiplication of the carrier vector and the data vector. Thus, it can be expressed as the addition of the I and Q components as follows:

$$
\begin{aligned}
&A_s \exp(j\varphi_s) \\
&= A_{sc} \exp(j\varphi_{sc}) \cdot A_m \exp(j\varphi_m) \\
&= A_s \exp(j\varphi_{sc}) \cos\varphi_m + jA_s \exp(j\varphi_{sc}) \sin\varphi_m.
\end{aligned} \tag{1}
$$

where the $A_s \exp(\varphi_s)$, $A_{sc} \exp(\varphi_{sc})$ and $A_m \exp(\varphi_m)$ are the optical vector, optical carrier and the data vector, respectively. Therefore, the so-called QD process for optical vector is to separate the data vector into I and Q components while maintaining the optical carrier part as shown in Fig. 1.
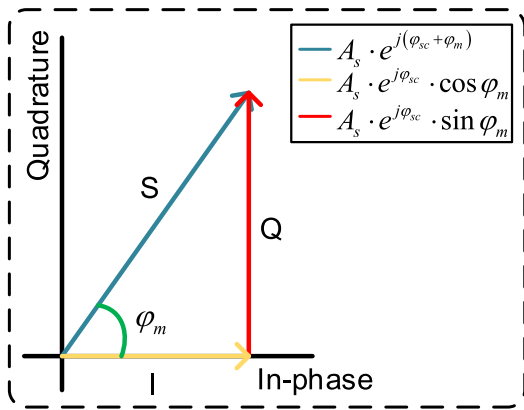

FIGURE 1. Concept map of the quadrature de-multiplexing process.

The schematic diagrams of the proposed QD structure, the on-chip solution and the corresponding signal spectra in the QD process are depicted in Fig. 2. (a)-(c), respectively. The input signal (Sig) and pump1 (P1) are combined together and then injected into the SOA in opposite directions after the coupler (cpl1). The four-wave mixing (FWM) effects among the injected waves occur in a bi-directional SOA like [34] and then the input signal and its conjugator (Idl) are output at different ports. With the separate signal and conjugator, the optical quadrature de-multiplexing can be accomplished by two-level degenerate PSA. The generation of conjugator was firstly proposed in [35]. Here we revise the configuration and nonlinear media to apply it to the optical vector QD.

As shown in Fig. 2. (a), the electrical fields of the launched signals at QD input ports A_1 and B_1 can be expressed as:

$$
\begin{bmatrix} A_1 \\ B_1 \end{bmatrix} = \begin{bmatrix} A_{p1} \exp(j\varphi_{p1}) + A_s \exp(j\varphi_s) \\ A_{p2} \exp(j\varphi_{p2}) \end{bmatrix}, \tag{2}
$$

where A_1 and B_1 are denoted in Fig. 2. (a) and the input signal $A_s \exp(j\varphi_s)$ is identical to the optical vector in equation (1). Then the signals after going through the coupler1 (cpl1) at the

ponits C_1 and D_1 have the expressions as:

$$
\begin{bmatrix} C_1 \\ D_1 \end{bmatrix} = \frac{1}{\sqrt{2}} \begin{bmatrix} A_{p1} \exp(j\varphi_{p1}) + A_s \exp(j\varphi_s) \\ +jA_{p2} \exp(j\varphi_{p2}) \\ jA_{p1} \exp(j\varphi_{p1}) + jA_s \exp(j\varphi_s) \\ +A_{p2} \exp(j\varphi_{p2}) \end{bmatrix}, \tag{3}
$$

The signals at C_1 and D_1 both have the components of P1, P2 and Sig and then are injected into the SOA in opposite directions. The FWM effects occur in SOA and the idler waves which are the input signal's conjugator are generated. The electrical fields at the points C_2 and D_2 can be expressed as:

$$
\begin{bmatrix} C_2 \\ D_2 \end{bmatrix} = \sqrt{\frac{G}{2}} \begin{bmatrix} A_{p1} \exp(j\varphi_{p1}) + A_s \exp(j\varphi_s) \\ +jA_{p2} \exp(j\varphi_{p2}) + jA_i \exp(j\varphi_i) \;// \\ jA_{p1} \exp(j\varphi_{p1}) + jA_s \exp(j\varphi_s) \\ +A_{p2} \exp(j\varphi_{p2}) + A_i \exp(j\varphi_i) \end{bmatrix}, \tag{4}
$$

where $\sqrt{G}$ is the amplitude gain of SOA and the $A_i \exp(j\varphi_i)$ is the idler generated in the FWM process. For the principle of FWM, the idler phase fulfills the relationship of $\varphi_i = \pi/2 + \varphi_{p1} + \varphi_{p2} - \varphi_s$. After the idler generated, the signals go through the cpl1 again and then the constructive and destructive interferences occur in the coupling process for the phase relationship between the signals which is shown in the third and fourth step in Fig. 2. (c). We can get the expressions of the signals at the points A_2 and B_2 as:

$$
\begin{bmatrix} A_2 \\ B_2 \end{bmatrix} = j\sqrt{G} \begin{bmatrix} A_{p1} \exp(j\varphi_{p1}) + A_s \exp(j\varphi_s) \\ A_{p2} \exp(j\varphi_{p2}) + A_i \exp(j\varphi_i) \end{bmatrix}, \tag{5}
$$

The Sig and its idler are separated into different nodes and directions, then they go through the circulators (Cirs) and optical band-pass filters (BPFs). The signals' electrical fields at the points G and H can be described as:

$$
\begin{bmatrix} G \\ H \end{bmatrix} = j\sqrt{G} \begin{bmatrix} A_s \exp(j\varphi_s) \\ A_i \exp(j\varphi_i) \end{bmatrix}, \tag{6}
$$

Then the Sig and idler are injected into the cpl2 to accomplish the phase sensitive amplification process which can be expressed as:

$$
\begin{bmatrix} I \\ Q \end{bmatrix} = j\sqrt{\frac{G}{2}} \begin{bmatrix} A_s \exp(j\varphi_s) + jA_i \exp(j\varphi_i) \\ jA_s \exp(j\varphi_s) + A_i \exp(j\varphi_i) \end{bmatrix}, \tag{7}
$$

Here we define $\theta = \pi/2 + \varphi_{p1} + \varphi_{p2} - 2\varphi_{sc}$ and m to be the amplitude ratio of the idler and Sig. The equation (7) can be derived as:

$$
\begin{bmatrix} I \\ Q \end{bmatrix} = \frac{j\sqrt{G} A_s \exp(j\varphi_{sc})}{\sqrt{2}} \begin{bmatrix} \exp(j\varphi_m) + jm \exp(j(\theta - \varphi_m)) \\ j\exp(j\varphi_m) + m \exp(j(\theta - \varphi_m)) \end{bmatrix}, \tag{8}
$$

We make the $m = 1$ by controlling the power ratio among P1, P2 and Sig and the nonlinear coefficient of SOA. The key point to realize the phase sensitive amplification process is to
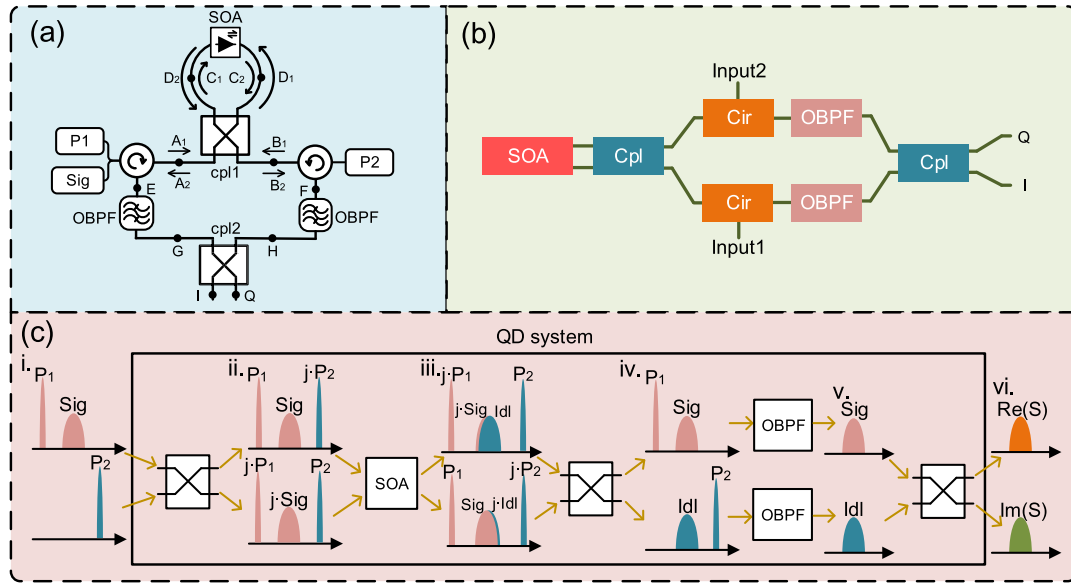
FIGURE 2. (a) QD system set-up; (b) schematic diagram for the on-chip QD; (c) spectrum schematic diagrams for the de-aggregation process in QD.

keep the θ to be a constant value such as:

$$\begin{bmatrix} I \\ Q \end{bmatrix} = \begin{cases} -\sqrt{2G}A_s \exp(j\varphi_{sc}) \begin{bmatrix} \sin\varphi_m \\ \cos\varphi_m \end{bmatrix} \\ \qquad (\theta = \pi/2 + 2n\pi) \,// j\sqrt{2G}A_s \exp(j\varphi_{sc}) \begin{bmatrix} \cos\varphi_m \\ -\sin\varphi_m \end{bmatrix} \\ \qquad (\theta = 3\pi/2 + 2n\pi), \end{cases} \tag{9}$$

where n is integer. In equation (9), when the $\theta = \pi/2 + 2n\pi$ or $\theta = 3\pi/2 + 2n\pi$, the data vector of the input signal is de-aggregated into I and Q components and the carrier vector is maintained like the equation (1) and the QD implements the quadrature de-multiplexing function for optical vector.

Moreover, under the condition of $\theta = 3\pi/2 + 2n\pi$, the output phase and power gain of I and Q components can be expressed as:

$$\varphi_I = \begin{cases} 2n\pi, & -\pi/2 \leq \varphi_m \pm 2n\pi < \pi/2 \\ (2n+1)\pi, & \pi/2 \leq \varphi_m \pm 2n\pi < 3\pi/2, \end{cases} \tag{10}$$

$$\varphi_Q = \begin{cases} \pi/2 \pm 2n\pi, & 0 \leq \varphi_m \pm 2n\pi < \pi \\ 3\pi/2 \pm 2n\pi, & \pi \leq \varphi_m \pm 2n\pi < 2\pi, \end{cases} \tag{11}$$

where the φ_I and φ_Q are the output phase of the signals at the I and Q output ports, respectively. We can see from equation (10) and (11) that the I and Q output ports of the QD are both a two-level degenerate PSA and they extract the I and Q components of the data vector in the phase domain, respectively.

$$G_{total} = \begin{cases} G_I = 10 \cdot \log\left(2G\cos^2\varphi_m\right) \\ G_Q = 10 \cdot \log\left(2G\sin^2\varphi_m\right). \end{cases} \tag{12}$$

The G_{total}, G_I and G_Q are the power gain of the whole QD system, QD I output and QD Q output, respectively. The equation (12) tells that the QD power gain is sensitive to the phase of input data vector and has a period of π.

The theoretical derivations show that the QD can implement the QD function for input data vector, while maintains the optical carrier basing on the 2-level bi-directional PSA. In the implementation of the QD, there are two practical issues should be considered. One is to prepare phase-coherent continuous waves (CWs) for the P1, P2 and carrier of Sig. The realization of the phase-sensitive amplification process relies on the condition that the phase of $\theta = \pi/2 + \varphi_{p1} + \varphi_{p2} - 2\varphi_{sc}$ is a constant value. For the moment, it is difficult to generate phase-coherent local pumps for an incoming signal with a free-running carrier. The optical frequency combs based pumps-generation scheme in [13] is a feasible solution for this problem. The other critical issue is to maintain the coherence of the CWs in the de-aggregation functioning process. It should be noted that the environment and device issues have great effects on the coherence among the CWs when the optical waves are transmitted along different paths. Active phase-locking devices or on-chip realization of QD could be a good solutions to this issue. From Fig. 2 (a), we can see that the signal and idler mostly share the same optical path in the proposed QD system except the paths from coupler1 to coupler2 where the active phase-locking devices should be added to maintain the phase condition of $\theta = \pi/2 + 2n\pi$ or $\theta = 3\pi/2 + 2n\pi$. Moreover, if the QD is realized on-chip, it can also effectively resist these issues.

III. SIMULATION AND DISCUSSION
The proposed QD scheme is verified by numerical simulations. As shown in Fig. 3, the input signal (wavelength:
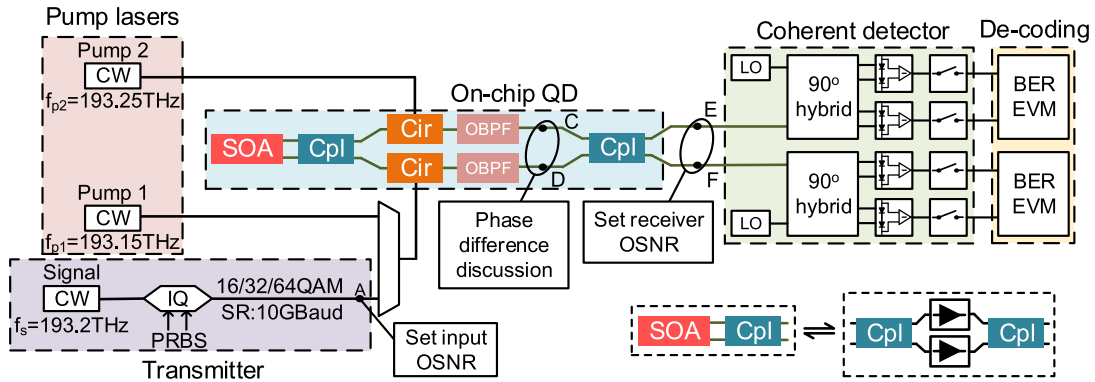
FIGURE 3. QD system setup for optical vector de-aggregation simulations.

193.2 THz, power: 0.8 mW), P1 (wavelength: 193.15 THz, power: 6 mW) and P2 (wavelength: 193.25 THz, power: 6 mW) are injected into the QD for the optical quadrature de-multiplexing process. The QD is constructed by two couplers (50:50), two circulators (3 ports), two band-pass filters (wavelength: 193.2 THz, bandwidth: 20 GHz) and a SOA. The SOA we employ is a traveling-wave SOA model introduced in [36] and the model parameters setting of the SOA are shown in Table 1. The model considered the stimulated emission, linear, bimolecular, and the Auger recombination and neglects the amplified spontaneous emission (ASE) noise. Moreover, the SOA in the QD is used as a bi-directional non-linear optical medum, so we built an equivalent structure for the bidirectional SOA by two traveling-wave SOAs which is shown in the bottom right corner of Fig. 3. Four kinds of input optical vector signals are injected into the QD to evaluate the system performance. A CW light with constant amplitude and an information phase range of $(-\pi/2, 5\pi/2)$ is injected into the QD to evaluate the system transfer characteristics. 16/32/64 QAM signals (symbol rate: 10 GBaud) are also injected into the QD to perform the QAM de-aggregations and the QAM signal input OSNR is set by adding amplifier spontaneous emission (ASE) noise at the point A. The ASE noise is also added at the points of E and F to control the
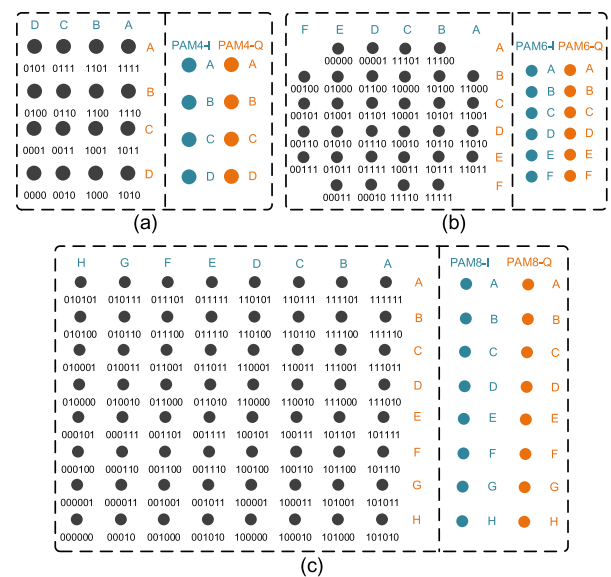
TABLE 1. Parameters setting of SOA.

Parameters Description	Symbol	Value
Inject current of SOA	I	650.0 mA
Length of the amplifier	L	600.0 μm
Width of the active layer	w	1.5 μm
Thickness of the active layer	d	18.0 nm
Confinement of the optical mode in the active region	Γ	0.15
Waveguide losses	α_s	40.0e2 m^{-1}
Differential gain	dg/dN	2.78e-20 m^2
The carrier density at transparency point	N_{tr}	1.4e-20 m^{-3}
Linewidth enhancement factor	α	5.0
Linear recombination coefficient	A	1.43e8 s^{-1}
Bimolecular recombination coefficient	B	1.0e-16 m^{3}s^{-1}
Auger recombination coefficient	C	3.0e-41 m^{6}s^{-1}
Initial carrier density		3.0e24 m^{-3}

FIGURE 4. QAM signals coding schemes and the corresponding relation for the signals before and after de-aggregations.

receiver OSNR for the de-aggregated signals. The QAM coding scheme and the corresponding relation for the signals before and after the QD which is also the receiving scheme are shown in Fig. 4. $2^{15} = 32768$ symbols are propagated through the QD to estimate the signal BER by Monte-Carlo method. Through the QD, the output signals are detected and analyzed to calculate the constellations, EVM and BER. Moreover, the effect of the phase difference is discussed and quantitatively analyzed by the BPF which reflects the signal BER performance under different path phase differences. When depicting the constellations and EVMs of the de-aggregations, the input OSNR of 16/32/64 QAM signals are set to be 17, 21 and 25 dB, respectively. When calculating the BERs and BPFs, the input OSNR of 16/32/64 QAM signals are all set to be 25 dB for the following unified analysis.

The constellations of the modulated CW signal after the QD are shown in Fig. 5 (a). We can see that input signal is squeezed into two lines through the QD. It reveals that
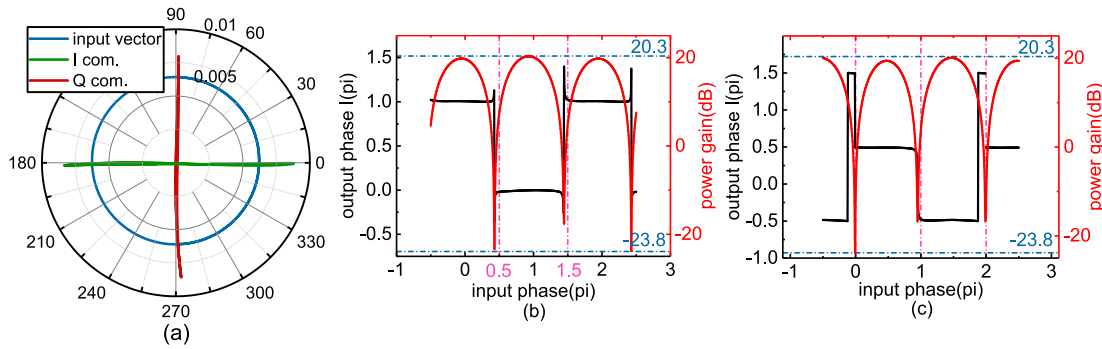
FIGURE 5. Transfer characteristics of the QD system.

the I and Q components are extracted separately from the input optical vector. The gain versus input-phase and output-phase versus input-phase characteristics of the I and Q ports are depicted in Fig. 5 (b) and (c), respectively. The phase transfer curves have a two-level stair-step shape which is consistent with equation (10)-(11) and indicates the nearly optimal two-level phase quantizing feature of degenerate PSA. We defined the gain extinction of the gain transfer curve to be the difference of the highest and lowest values of the PSA gain to input-phase transfer curves depicted in Fig. 5 (b) and (c). Because of the gain and high non-linear effects of the SOA, the SOA-based PSA has a relative high phase-sensitive extinction gain ratio of 44.1dB in both quadrature components which is expressed by equation (12). The PSA proposed in [30] and [31] show the phase-sensitive extinction gain ratio values of their PSA systems are 6.5 dB and 11.1 dB, respectively which can be applied in regenerating BPSK signals while may not suitable for quadrature de-multiplexing. The phase-sensitive gain extinction ratio is an important indicator which shows the performance of quadrature de-multiplexing function. The quadrature de-multiplexing of the QD is accomplished by amplifying the quadrature part we want while attenuating the other one. The value of the phase-sensitive gain extinction is larger, the performance of the quadrature de-multiplexing function is better. Specially, for one QD system, the lowest point of the gain transfer curve must be negative to guarantee that the unwanted quadrature of input optical vector is attenuated.

The constellations and the corresponding EVMs of the input and output signals in the QAM de-aggregations are depicted in Fig. 6. The constellations and EVM of 16/32/64 QAM signals are performed at the point A in Fig. 3 for the input signals with OSNR of 17, 21 and 25dB respectively. The signals before being added ASE noise at the points of E and F in Fig. 3 are detected to evaluate constellations and EVM for the signals after de-aggregations. The constellations visually tells that the input 16/32/64 QAM signals are de-aggregated into two PAM 4/6/8 signals, indicating the QD simultaneously extracts the I and Q components for input optical vector. From the perspective of EVM,

the de-aggregated PAM8 signals have a little higher EVM than the input 64QAM signal (about 1%) and the extracted PAM4 signals have better EVM performances than 16QAM signal. The PSA has the characteristics of phase-squeezing and phase-to-amplitude noise conversion. When the input signal has large input noise like the 16QAM signal, the phase-squeezing characteristic plays a major role in the QD process while the phase-to-amplitude noise conversion characteristic plays a decisive role for the high quality input signal like the 64QAM signal. Moreover, the extracted I and Q components have nearly the same EVM performance of each de-aggregation. Specially, the output PAM signals here are not totally the conventional PAM signals for they have two information-phase status and multi-amplitude levels which can be viewed as the combination of phase shift keying modulation and conventional PAM. The combination of the two modulation technologies leads that this kind of PAM signals have better anti-noise performance comparing with the conventional PAM signals while more complicated detection scheme is needed like cascading an optical delay interferometer and a photo-detector. The QD system we propose is to give a possible solution for an on-chip QD system to accomplish the all-optical quadrature de-multiplexing function. The input QAM signals are employed to verify the quadrature de-multiplexing function of the QD and they can be viewed as the special cases of optical vectors.

To evaluate the QD system performance quantitatively, the signals BER are estimated and depicted in Fig. 7 for the input 16/32/64 QAM signals and their corresponding de-aggregated PAM 4/6/8 signals. The de-aggregated PAM signals are received by the de-coding schemes in Fig. 4 and the BER performances show that they are validly detected which verifies that the QD completes the quadrature de-multiplexing function and the QD theoretical scheme is feasible. The PAM signals show superior BER performances comparing with the QAM signals. As shown in Fig. 7, under the input OSNR of 25 dB, the de-aggregated PAM 4/6/8 signals get 6.1 dB, 5.6 dB and 8.2 dB receiver OSNR improvements at the BER of 10^{-3}. Moreover, for each of the input QAM formats, the BER versus receiver OSNR curves of the PAM-I and PAM-Q signals almost stick together which proves that
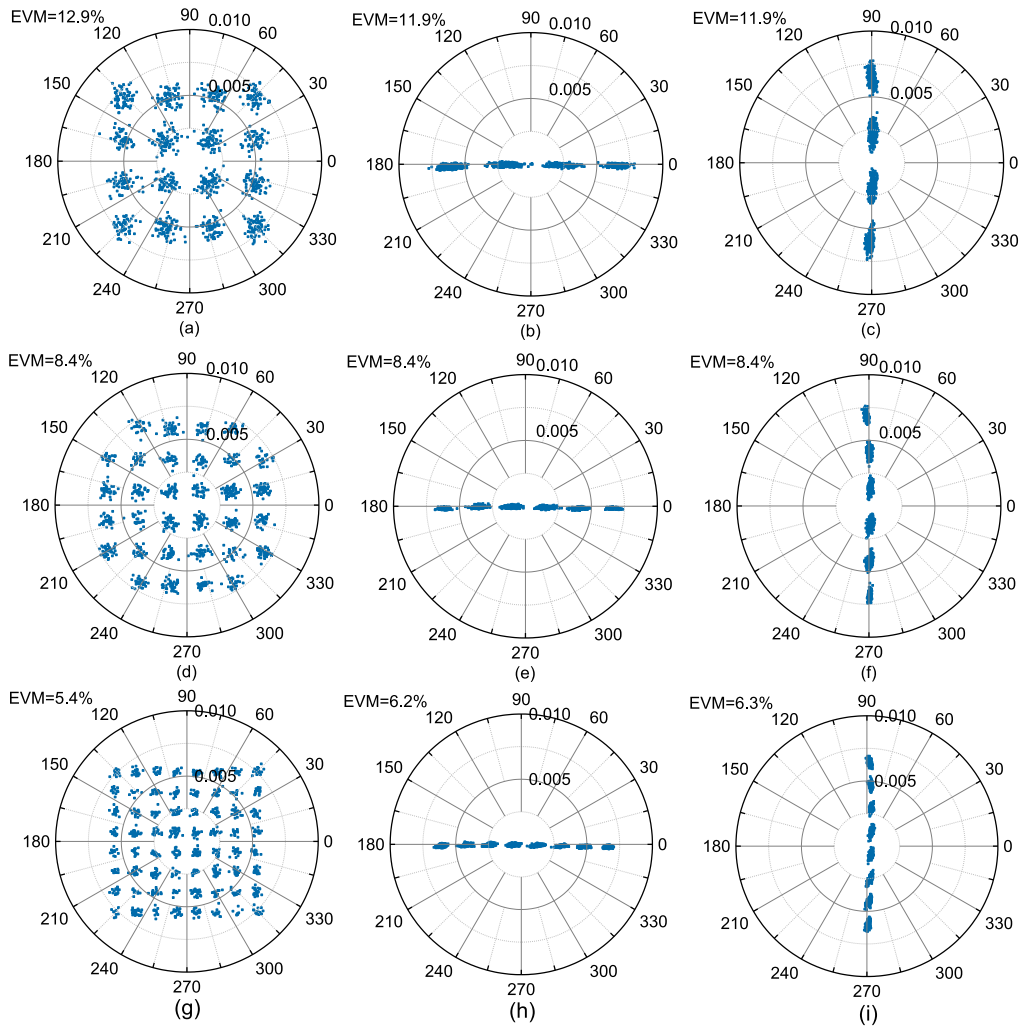
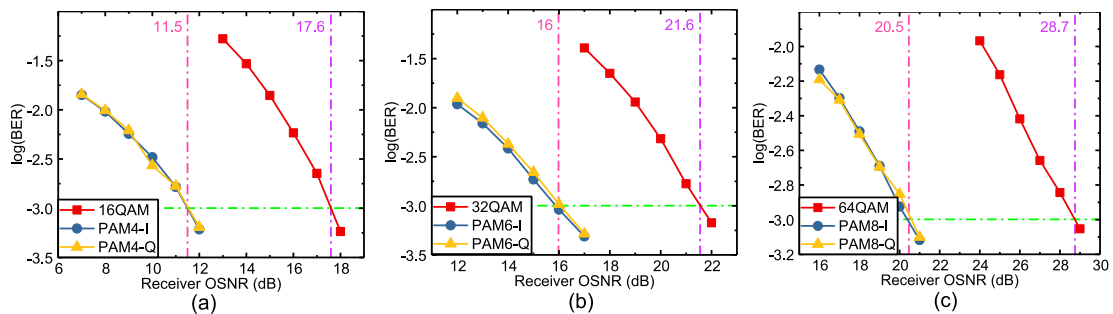**FIGURE 6.** Constellations and EVMs for QD process.

FIGURE 7. BER vs. receiver OSNR curves of QAM and PAM signals.

the I and Q components also have nearly the same BER performance.

We have mentioned that the environment and device issues have great effects on the system performance. As shown in Fig. 2 (a), the QD accomplishes the de-aggregations by injecting the Sig and its idler into the coupler2 and we assume

that their carriers are coherent. In the QD process, from the SOA to the coupler1, the Sig and idler share the same path and this issue can be neglected. While from the coupler1 to the coupler2, the Sig and idler are transmitted through different paths so the following coupling is under the influence of the environment and device issues. To investigate the influence
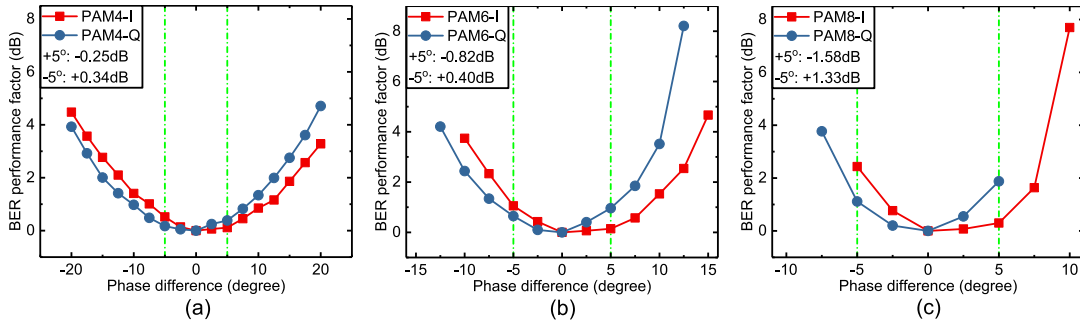
FIGURE 8. BER performance factor vs. path phase difference of de-aggregated PAM signals.

of environment and device, variable phase shifts are added at the points C and D in Fig. 3 and the signal BER performances under different system phase differences are estimated. Furthermore, BPF are defined as:

$$BPF = 10 \log \frac{OSNR_d}{OSNR_0}. \tag{13}$$

where $OSNR_0$ and $OSNR_d$ are the signal receiver OSNRs at the BER of 10^{-3} of the signals with the phase difference of 0 and d, respectively. The extra phase shifts are marked to be positive when they are added at the point C, otherwise they are marked to be negative. BPF represents the signal BER performance in the system with the phase shift of d. A higher BPF means the system has worse BER performance due to the environment and device influences.

Fig. 8 depicts the BPFs under different phase differences for the de-aggregated PAM signals. We can see that all the de-aggregated PAM signals have the lowest BPF at the phase difference of 0 degree which verifies that the extra phase shift deteriorates the system performance. As shown in Fig. 8, when the phase difference is set to be positive, the de-aggregated signals in I branches have better BER performance than the signals in Q branches, whereas the Q components are better than I components. Under the phase difference of 5 degree, the BPFs of I components are 0.25 dB, 0.82 dB and 1.58 dB lower than that of the Q components for the de-aggregated PAM 4/6/8 signals, respectively. Moreover, the BPFs of Q components are 0.34 dB, 0.4 dB and 1.33 dB better than that of the I components when the phase difference is -5 degree. The difference between the two branches signifies that the system phase difference has a bad influence on the BER performance of the I and Q components symmetrically. The BER performance symmetry of higher-order format signal is more sensitive to the phase difference than that of lower-order format signals.

To further analyze the effects of the system phase difference, we sort the BPF data of the de-aggregated signals into I and Q branches and replot them in Fig.8. As depicted in Fig. 9, when the BPF is 2 dB, the span of the phase difference are 27.5 degree, 17.8 degree and 11.9 degree for the PAM 4/6/8 in I branch, respectively. In Q branch, the span are 27.5 degree, 16.9 degree and 10.8 degree for PAM 4/6/8,
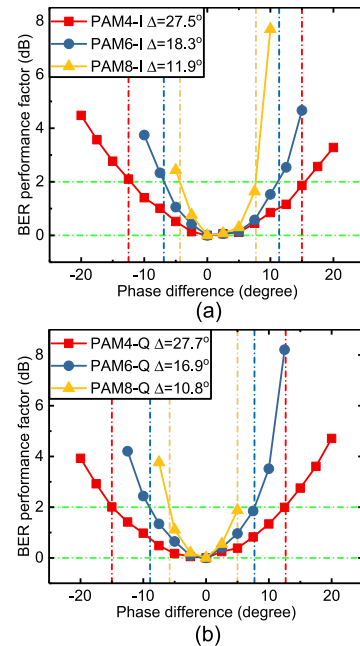

FIGURE 9. Comparisons of BER performance factor vs. path phase difference curves among different formats.

respectively under the BPF of 2 dB. All the curves are with a shape like a trough and the curve of higher-order format signal has narrower troughs in both I and Q components which reveals that the phase difference has more influence on the higher-order format signal BER performance. We can conclude that the system phase difference has effects on the signal BER performance with symmetry between I and Q branches. The higher-order format signal is more sensitive to the system phase difference.

IV. CONCLUSION
A simple optical vector QD scheme is proposed in this paper and the quadrature de-aggregations for 16/32/64 QAM signals are performed. The proposed QD unit contains single-stage degenerate phase sensitive amplification process and maintains the wavelength and polarization status of the extracted I and Q components the same as the input optical

vector. The constructing devices for the QD are all ready for on-chip integrations and thus enables a possible solution for on-chip QD system. For 10 Gbaud 16/32/64 QAM signals with input OSNR of 25 dB, the de-aggregated PAM4/6/8 signals show 6.1 dB, 5.6 dB and 8.2 dB receiver OSNR improvements at the BER of 10^{-3}. The constellations, EVMs and BERs of the QAM de-aggregations reveal that the QD is well-qualified for the optical vector quadrature de-multiplexing and has excellent system performances. The discussions on the BPF versus phase difference tell that the environment issues have serious influence on the system BER performance and the BER performance symmetry between the de-aggregated I and Q components. The proposed QD has considerable potential in future flexible AON such as the information de-aggregation and format conversion and optical vector direct detection.

ACKNOWLEDGMENT

REFERENCES
[1] Y. Ji, J. Zhang, X. Wang, and H. Yu, "Towards converged, collaborative and co-automatic (3C) optical networks," *Sci. China Inf. Sci.*, vol. 61, no. 12, p. 121301, Dec. 2018.

[2] Y. Ji *et al.*, "Prospects and research issues in multi-dimensional all optical networks," *Sci. China Inf. Sci.*, vol. 59, no. 10, p. 101301, 2016.

[3] A. E. Willner, "All-optical signal processing techniques for flexible networks," in *Proc. Conf. Opt. Fiber Commun. Exhib.*, 2018, pp. 1–47, Paper W3E.5.

[4] J. Yu *et al.*, "8× 506-Gb/s 16 QAM WDM signal coherent transmission over 6000-km enabled by PS and HB-CDM," in *Proc. Conf. Opt. Fiber Commun. Exhib.*, 2018, pp. 1–3, Paper M2C-3.

[5] K. Kasai *et al.*, "Single-carrier 552 Gbit/s, 46 Gbaud 64 QAM coherent transmission over 100 km with co-propagating 10 Gbit/s-OOK signals through a deployed ROADM network," in *Proc. Eur. Conf. Opt. Commun.*, 2017, pp. 1–3.

[6] A. Matsushita, M. Nakamura, F. Hamaoka, and Y. Kisaka, "Single-carrier 48-GBaud PDM-256 QAM transmission over unrepeated 100 km pure-silica-core fiber using commercially available μITLA and LN-IQ-modulator," in *Proc. Conf. Opt. Fiber Commun. Exhib.*, 2018, pp. 1–3, Paper M1C.1.

[7] F. Da Ros *et al.*, "Dual-polarization wavelength conversion of 16-QAM signals in a single silicon waveguide with a lateral p-i-n diode [Invited]," *Photon. Res.*, vol. 6, no. 5, pp. B23–B29, 2018.

[8] S. Zheng *et al.*, "Demonstration of on-chip 640-Gbit/s throughput, granularity-flexible programmable optical filtering and reconfigurable optical add/drop multiplexing on silicon platform," in *Proc. Conf. Opt. Fiber Commun. Exhib.*, 2018, pp. 1–3, Paper Th3C-4.

[9] R. Konoike *et al.*, "Lossless operation of SOA-integrated silicon photonics switch for 8× 32-Gbaud 16-QAM WDM signals," in *Proc. Conf. Opt. Fiber Commun. Exhib.*, 2018, pp. 1–3, Paper Th4B.6.

[10] P. Liao *et al.*, "Effects of erbium-doped fiber amplifier induced pump noise on soliton Kerr frequency combs for 64-quadrature amplitude modulation transmission," *Opt. Lett.*, vol. 43, no. 11, pp. 2495–2498, 2018.

[11] T. Umeki *et al.*, "Polarization-diversity in-line phase sensitive amplifier for simultaneous amplification of fiber-transmitted WDM PDM-16 QAM signals," in *Proc. Conf. Opt. Fiber Commun. Exhib.*, 2018, pp. 1–3, Paper M3E–4.

[12] M. Gao, T. Kurosu, T. Inoue, and S. Namiki, "Low-penalty phase de-multiplexing of QPSK signal by dualpump phase sensitive amplifiers," in *Proc. Eur. Conf. Opt. Commun.*, 2013, pp. 1–3, Paper We.3.A.5.

[13] F. Da Ros, K. Dalgaard, L. Lei, J. Xu, and C. Peucheret, "QPSK-to-2× BPSK wavelength and modulation format conversion through phase-sensitive four-wave mixing in a highly nonlinear optical fiber," *Opt. Express*, vol. 21, no. 23, pp. 28743–28750, 2013.

[14] A. Lorences-Riesgo *et al.*, "Quadrature demultiplexing using a degenerate vector parametric amplifier," *Opt. Express*, vol. 22, no. 24, pp. 29424–29434, 2014.

[15] M. Ziyadi *et al.*, "Tunable optical de-aggregation of a 40-Gbit/s 16-QAM signal into two 20-Gbit/s 4-PAM signals using a coherent frequency comb and nonlinear processing," in *Proc. Conf. Lasers Electro-Opt.*, 2016, pp. 1–2, Paper SM3F–5.

[16] A. Lorences-Riesgo, T. A. Eriksson, M. Mazur, P. A. Andrekson, and M. Karlsson, "Quadrature decomposition of a 20 Gbaud 16-QAM signal into 2 × 4-PAM signals," in *Proc. Eur. Conf. Opt. Commun.*, 2016, pp. 1–3, Paper Tu.1.E.3.

[17] A. Fallahpour *et al.*, "Experimental demonstration of tunable optical de-aggregation of each of multiple wavelength 16-QAM channels into two 4-PAM channels," in *Proc. Conf. Opt. Fiber Commun. Exhib.*, 2017, pp. 1–3, Paper Th4I.6.

[18] H. Kishikawa, N. Goto, and L. R. Chen, "All-optical wavelength preserved modulation format conversion from PDM-QPSK to PDM-BPSK using FWM and interference," *J. Lightw. Technol.*, vol. 34, no. 23, pp. 5505–5515, Dec. 1, 2016.

[19] R. Slavík *et al.*, "All-optical phase and amplitude regenerator for next-generation telecommunications systems," *Nature Photon.*, vol. 4, no. 10, pp. 690–695, 2010.

[20] J. Chen, L. Liu, and Y. Shi, "A polarization-insensitive dual-wavelength multiplexer based on bent directional couplers," *IEEE Photon. Technol. Lett.*, vol. 29, no. 22, pp. 1975–1978, Nov. 15, 2017.

[21] L. Liu *et al.*, "Low-power all-optical microwave filter with tunable central frequency and bandwidth based on cascaded opto-mechanical microring resonators," *Opt. Express*, vol. 25, no. 15, pp. 17329–17342, 2017.

[22] Z. Shen *et al.*, "Reconfigurable optomechanical circulator and directional amplifier," *Nature Commun.*, vol. 9, no. 1, p. 1797, 2018.

[23] M. Pinto, L. F. Marzall, A. Ashley, D. Psychogiou, and Z. Popović, "A design approach for monolithically integrated broadband circulators," in *Proc. Int. Appl. Comput. Electromagn. Soc. Symp. (ACES)*, 2018, pp. 1–2.

[24] X. Pommarede *et al.*, "16 × 100 GHz echelle grating-based wavelength multiplexer on silicon-on-insulator platform," *IEEE Photon. Technol. Lett.*, vol. 29, no. 6, pp. 493–495, Mar. 15, 2017.

[25] W. Liu *et al.*, "A fully reconfigurable photonic integrated signal processor," *Nature Photon.*, vol. 10, no. 3, pp. 190–195, 2016.

[26] J. Tang *et al.*, "Integrated optoelectronic oscillator," *Opt. Express*, vol. 26, no. 9, pp. 12257–12265, 2018.

[27] B. Yao *et al.*, "Gate-tunable frequency combs in graphene–nitride microresonators," *Nature*, vol. 558, pp. 410–414, Jun. 2018.

[28] W. Dong, Z. Huang, J. Hou, R. Santos, and X. Zhang, "Integrated all-optical programmable logic array based on semiconductor optical amplifiers," *Opt. Lett.*, vol. 43, no. 9, pp. 2150–2153, 2018.

[29] J. Cui, G.-W. Lu, H. Wang, L. Bai, and Y. Ji, "Single-stage phase-sensitive amplifier based quadrature de-multiplexer for de-aggregating QAM signals into in-phase and quadrature components," in *Proc. Conf. Lasers Electro-Opt.*, 2018, pp. 1–2, Paper JTu2A–36.

[30] L. A. Coldren *et al.*, "Single-chip dual-pumped SOA-based phase-sensitive amplifier at 1550 nm," in *Proc. IEEE Summer Topicals Meeting Ser. (SUM)*, Jul. 2015, pp. 88–89.

[31] G.-W. Lu *et al.*, "Experimental investigation of phase-sensitive amplification in quantum-dot semiconductor optical amplifier," in *Proc. Conf. Lasers Electro-Opt.*, 2016, pp. 1–2, Paper STu3G.5.

[32] A. D. Ellis and S. Sygletos, "Phase sensitive signal processing using semiconductor optical amplifiers," in *Proc. Conf. Opt. Fiber Commun. Exhib.*, 2013, pp. 1–3, Paper OW4C.1.

[33] K. R. H. Bottrill, R. Kakarla, F. Parmigiani, D. Venkitesh, and P. Petropoulos, "Phase regeneration of QPSK signal in SOA using single-stage, wavelength converting PSA," *IEEE Photon. Technol. Lett.*, vol. 28, no. 2, pp. 205–208, Jan. 15, 2015.

[34] H. Schmeckebier *et al.*, "Ultra-broadband bidirectional dual-band ouantum-dot semiconductor optical amplifier," in *Proc. Conf. Opt. Fiber Commun. Exhib.*, 2015, pp. 1–3, Paper Tu3I.7.

[35] H. C. Lim, F. Futami, and K. Kikuchi, "Polarization-independent, wavelength-shift-free optical phase conjugator using a nonlinear fiber Sagnac interferometer," *IEEE Photon. Technol. Lett.*, vol. 11, no. 5, pp. 578–580, May 1999.

[36] M. J. O'Mahony, "Semiconductor laser optical amplifiers for use in future fiber systems," *J. Lightw. Technol.*, vol. 6, no. 4, pp. 531–544, Apr. 1988.

JIABIN CUI received the B.S. degree from Harbin Engineering University, in 2014. He is currently pursuing the Ph.D. degree with the State Key Laboratory of Information Photonics and Optical Communications, School of Information and Communication Engineering, Beijing University of Posts and Telecommunications. His research interest focuses on all-optical signal processing.

HONGXIANG WANG received the Ph.D. degree in electromagnetic field and microwave technology from the Beijing University of Posts and Telecommunications, in 2005, where he is currently a Professor with the School of Information and Communication Engineering. His research interests are focused on all optical signal processing in optical communications and networks.

GUO-WEI LU (M'05) received the Ph.D. degree in information engineering from The Chinese University of Hong Kong (CUHK), Hong Kong, in 2005. From 2005 to 2006, he was a Post-Doctoral Fellow with CUHK. From 2006 to 2009, he was an Expert Researcher with the National Institute of Information and Communications Technology (NICT), Tokyo, Japan. From 2009 to 2010, he was an Assistant Professor with the Chalmers University of Technology, Gothenburg, Sweden. From 2010 to 2014, he was a Researcher with NICT. Since 2014, he has been with Tokai University as an Associate Professor. He has authored or co-authored over 180 peer-reviewed journal and conference publications. His current research interests include advanced optical modulation formats, photonic signal processing, and optical parametric amplifiers.

YUEFENG JI is currently a Professor and the Executive Deputy Director of the State Key Laboratory of Information Photonics and Optical Communications, Beijing University of Posts and Telecommunications, China. His research interests include broadband communication networks and optical communications, with emphasis on key theory, realization of technology, and application. He is a Fellow of the China Institute of Communications, The Chinese Institute of Electronics, and The Institution of Engineering and Technology.

• • •